



Evolution of ply cracks in multidirectional composite laminates

Chandra Veer Singh, Ramesh Talreja *

Department of Aerospace Engineering, Texas A&M University, College Station, TX 77843-3141, USA

ARTICLE INFO

Article history:

Received 1 May 2009

Received in revised form 15 December 2009

Available online 25 January 2010

Keywords:

Multidirectional composites

Ply cracking

Damage mechanics

Computational simulation

Damage evolution

ABSTRACT

This paper treats evolution of ply cracks in multidirectional composite laminates subjected to a quasi-static tensile load in the longitudinal direction. Starting with pre-existing ply cracks in off-axis plies, the formation of additional cracks is analyzed by an energy-based approach. A critical laminate energy parameter associated with formation of these cracks is defined and is evaluated using experimental data for a reference cross-ply laminate. The modeling approach requires crack surface displacements, which are calculated by a three-dimensional finite element (3-D FE) analysis performed on a suitable representative volume of the given cracked laminate. The model predictions agree well with experimental data for $[0/\pm\theta_4/0_{1/2}]_s$ and $[0/90/\mp 45]_s$ laminates. A parametric study is conducted to evaluate effects of ply thickness and ply stacking sequence on damage evolution in $[0_m/90_n/\mp\theta_p]_s$ laminates.

© 2010 Elsevier Ltd. All rights reserved.

1. Introduction

Composite laminates with plies oriented in multiple directions are common in practical applications. Although fibers are often placed along a major load direction, other orientations are needed to meet strength and rigidity requirements under transverse and shear loadings. One scenario of interest in design of multidirectional laminates consists of cracks in plies with fibers inclined to an axis of symmetry. Such cracks are termed off-axis ply cracks, and in the case when the off-axis angle is 90° , they are called transverse cracks. The problem of transverse cracks in cross-ply laminates is perhaps the most studied problem in damage of composite materials, while other off-axis cases have posed a much greater challenge. The difficulty lies in the three-dimensionality of the problem, except for the transverse cracks where a two-dimensional treatment suffices. We have addressed the stiffness degradation of laminates with off-axis cracks of fixed mutual spacing elsewhere (Singh and Talreja, 2008, 2009); here the focus is on the evolution of these cracks. The full problem of developing constitutive relationships for composites with damage can be addressed by combining stiffness degradation and evolution solutions.

Experimental studies of off-axis ply cracks are also fewer than those of transverse cracks. We will consider the data reported in Crocker et al. (1997), Tong et al. (1997) and Varna et al. (1999). Although the observations reported in these studies indicate the

presence of some delamination, we will treat only ply cracks and assess our predictions against the reported data.

Previous damage evolution studies have mostly considered transverse cracks. As discussed for instance in a review by Nairn (2000), the approaches may be categorized as strength-based or energy-based. In the former, one assumes formation of new cracks when the maximum normal stress between two pre-existing adjacent cracks in apply reaches a critical (strength) value. The energy-based approaches are guided by fracture mechanics concepts, and a most common criterion used is the Griffith criterion for brittle fracture with the critical energy release rate often modified in some manner (Nairn, 2000). Nairn et al. (1993) found that the prediction of the strength-based approaches did not consistently agree with experimental data. The energy-based approach combined with probabilistic considerations (Vinogradov and Hashin, 2005) match well the data for transverse cracks in cross-ply laminates.

The stress analysis of cracked laminates needed in damage evolution is generally a complex task. In the special case of transverse cracks in cross-ply laminates, a reasonably accurate evaluation of local stresses is possible, e.g. by the variational analysis (Vinogradov and Hashin, 2005). However, for other off-axis ply cracking cases, the three-dimensionality of the problem makes a numerical analysis inevitable. Alternatively, approximate stress analysis by some modification of the basically one-dimensional shear-lag analysis can be employed, such as in Kashtalyan and Soutis (2006) for angle-ply cracks and in Yokozeki et al. (2005) for obliquely crossed cracks.

We will here adopt an energy-based approach for off-axis ply cracks. One specific laminate we will consider is $[0/\pm\theta_4/0_{1/2}]_s$ with cracks of equal density in the $\pm\theta$ plies, as we have treated this

* Corresponding author. Tel.: +1 979 458 3256; fax: +1 979 845 6051.

E-mail addresses: chandraveer@tamu.edu (C.V. Singh), talreja@aero.tamu.edu (R. Talreja).

case for stiffness degradation (Singh and Talreja, 2008) and experimental data for this case is also available (Varna et al., 1999). The other case is $[0/90/\mp 45]_s$ laminate for which experimental data have been reported in Tong et al. (1997). Finally, to gain further insight into the behavior of off-axis ply cracking, we will conduct a study of $[0_m/90_n/\mp \theta_p]_s$ laminates with ply thickness as a parameter, studying effects of stacking sequence change to some extent as well.

2. Off-axis ply cracking and energy-based analysis

Before treating off-axis ply cracking let us briefly review the transverse cracking process. The formation and progression of transverse cracks in cross-ply laminates have been the objects of numerous studies, ranging from experimental to analytical/computational; for a recent review, see Berthelot (2003). Experimental observations indicate that in formation of a transverse crack, fiber/matrix interfacial debonding and matrix cracking are involved. Such a crack is found generally to span the ply thickness before growing in the laminate width direction. Furthermore, on increasing the applied load, the number of transverse cracks is found to increase by formation of new cracks a certain distance away from the previously formed cracks. In the initial stages, the crack multiplication process results in non-uniform spacing between cracks, but the spacing becomes increasingly uniform as cracks come closer. In continuum modeling, one smears out the heterogeneous microstructure of plies, replacing them with homogeneous, orthotropic layers, and places transverse cracks in the 90° layers with crack fronts (edges) at the $90^\circ/0^\circ$ interfaces and the crack planes extending through the laminate width. This scenario (geometric model) is the basis for most stress analyses as well as for estimates of overall laminate stiffness changes.

A range of studies of transverse cracks have been concerned with the formation of a crack in the 90° plies of a cross-ply laminate, seeking to determine at what applied load this occurs. An approach, commonly described as strength-based, assumes that the crack forms when the stress normal to fibers in the 90° plies reaches a critical value. Realizing that crack formation requires creation of two surfaces by failure (cleavage) over a plane, a point-failure criterion is only meaningful if all points over a potential crack plane attain the critical stress simultaneously. This condition can be reasonably assumed if the normal stress under consideration is uniformly distributed over that plane. In relatively thick 90° plies the axial normal stress throughout the plies in the uncracked state,

as well as along planes midway between pre-existing transverse cracks in the cracked state, is approximately uniform. Thus, a strength-based criterion for transverse crack formation will be a good approximation in this case. For thin transverse plies, however, a different approach is needed. One such approach has been described as energy-based, deriving this characterization from the familiar strain energy release rate concept of fracture mechanics. Here one assumes a crack (or flaw) to already exist along the anticipated new crack plane. The object of analysis is the growth of this crack. Different analyses result depending on what growth scenario is assumed. In a common scenario the crack is viewed as growing through the ply thickness towards the $90^\circ/0^\circ$ interfaces. In analyzing this case within the context of a two-dimensional stress analysis a somewhat unrealistic crack of infinite dimension along the laminate width but of small dimension in the thickness direction is assumed. One then examines the instability of growth of such a crack, applying usually the Griffith criterion for brittle fracture (unstable crack growth when energy release rate associated with advancement of the crack front equals a critical value). Alternatively, the crack is assumed to have grown fully between the $90^\circ/0^\circ$ ply interfaces and its growth along the laminate width is examined. A crack advancing in this mode has been given an imaginative name of *tunneling crack* and several studies have looked at the criticality of this mode. One study has compared the two scenarios and found that the tunneling growth mode in typical composites is less critical than the crack growth towards the $0^\circ/90^\circ$ interfaces (Yang et al., 2003).

The material parameters entering in the studies of transverse crack formation are tensile strength normal to fibers in a ply (in the strength-based approach) and the fracture toughness associated with crack growth along fibers in a unidirectional ply (in the energy-based approach). These parameters are useful in material selection.

When the purpose is to construct constitutive relationships for composite laminates undergoing damage, as is the case here, the damage evolution analysis should be consistent with the analysis of stiffness changes due to damage. Thus, the state of damage defined in stiffness–damage relationships, such as in Singh and Talreja (2008) for off-axis cracking, should also be the state considered for evolution. This will be discussed next.

As depicted in Fig. 1, a tensile load is applied along a symmetry axis of a laminate, which in a general case has plies along this direction as well as in other directions inclined to it. The load induces in an off-axis ply a stress state, which has in-plane compo-

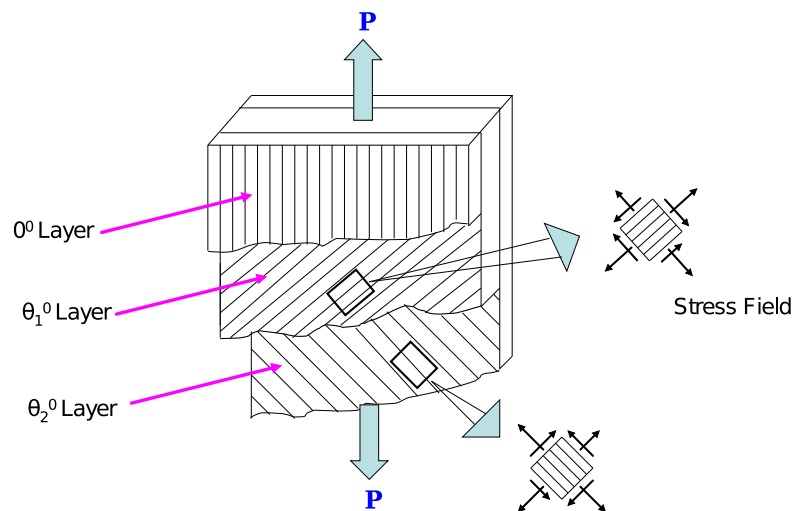


Fig. 1. An off-axis laminate loaded in axial tension.

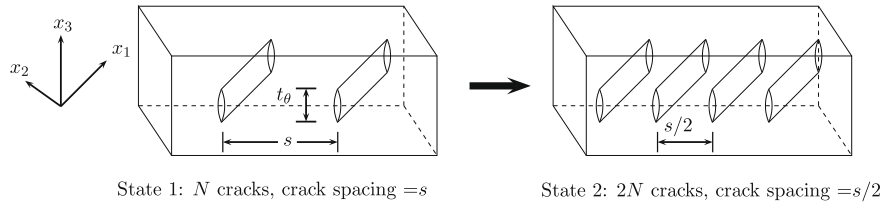


Fig. 2. Progressive multiplication of ply cracks.

nents, as indicated in the figure. Under suitable conditions, this stress state may cause cracks to form along fibers in the ply. The damage state considered for stiffness changes induced by such cracks, as well as for its evolution, consists of a set of parallel intra-laminar cracks with a constant mutual spacing. Fig. 2(left) depicts two adjacent cracks of spacing s from the set of N cracks in a representative volume element of the laminate. Let us denote this arbitrary damage state by State 1, as indicated in the figure. On increasing the applied load to a suitable level, additional cracks form midway between two existing cracks, increasing the number of cracks from N to $2N$ and reducing the mutual spacing to $s/2$, as indicated in Fig. 2(right). Since the selection of the value of s is arbitrary, it defines a continuous damage state variable. We shall here analyze the evolution of this damage variable (or, equivalently, its reciprocal, the linear crack density) with the applied load. This analysis is based on energy considerations, and is described next.

Let the damage state of N cracks (State 1) with crack spacing s evolve into State 2 of $2N$ cracks with crack spacing $s/2$ when the applied remote stress on the laminate reaches σ_{X0} . Taking all ply cracks to be brittle, it is reasonable to assume that State 2 is reached when the energy needed to form N new cracks in the presence of pre-existing N cracks becomes available from the deformed laminate under applied stress σ_{X0} . This energy is equal to the work performed in closure of the new crack planes, according to Irwin (1958). Following Joffe et al. (2001), we denote this work as W_{2N-N} , and assume, as they do, that this quantity can be calculated by using the identity

$$W_{2N-0} = W_{2N-N} + W_{N-0} \tag{1}$$

i.e. the work to close all $2N$ cracks is the sum of the work to close the N “new” cracks and the work to close the N “old” cracks, all under the applied stress σ_{X0} .

The work to close N off-axis cracks consists of the sum of the work performed by the tractions in closing crack opening displacement (COD) and in reversing crack sliding displacement (CSD). Thus, per unit laminate width, this work is given by,

$$W_{N-0} = 2 \cdot N \cdot \frac{1}{\sin \theta} \cdot \frac{1}{2} \int_{-t_\theta/2}^{t_\theta/2} \sigma_{20}^\theta u_n(x_3) dx_3 + 2 \cdot N \cdot \frac{1}{\sin \theta} \cdot \frac{1}{2} \int_{-t_\theta/2}^{t_\theta/2} \sigma_{120}^\theta u_t(x_3) dx_3 = N \cdot \frac{1}{\sin \theta} \cdot t_\theta \cdot [\sigma_{20}^\theta \cdot \bar{u}_n^\theta(s) + \sigma_{120}^\theta \cdot \bar{u}_t^\theta(s)] \tag{2}$$

where $\bar{u}_n^\theta(s)$ and $\bar{u}_t^\theta(s)$ are COD and CSD averaged over the surfaces of an off-axis crack of inclination θ measured from the loading axis, lying within a periodic array of cracks with spacing s , and t_θ is the thickness of the cracked ply (Fig. 2). The ply stress σ_{20}^θ is the unperturbed stress (i.e. in the undamaged state) normal to the crack plane and σ_{120}^θ is the associated shear stress, both stresses corresponding to the remotely applied laminate stress σ_{X0} .

It is useful to write the average COD and CSD variables in non-dimensionalized forms in order to obtain convenient relations between crack spacing s and the applied laminate stress (or strain). The normalized forms are chosen as

$$\bar{u}_n^\theta = \frac{\bar{u}_n^\theta}{t_\theta (\sigma_{20}^\theta / E_2)}; \quad \bar{u}_t^\theta = \frac{\bar{u}_t^\theta}{t_\theta (\sigma_{120}^\theta / E_2)} \tag{3}$$

Eq. (2) is now rewritten as

$$W_{N-0} = N \cdot \frac{1}{\sin \theta} (t_\theta)^2 \cdot \frac{1}{E_2} [(\sigma_{20}^\theta)^2 \cdot \bar{u}_n^\theta(s) + (\sigma_{120}^\theta)^2 \cdot \bar{u}_t^\theta(s)] \tag{4}$$

Similarly, the work to close $2N$ cracks of spacing $s/2$ is

$$W_{2N-0} = 2N \cdot \frac{1}{\sin \theta} (t_\theta)^2 \cdot \frac{1}{E_2} [(\sigma_{20}^\theta)^2 \cdot \bar{u}_n^\theta(\frac{s}{2}) + (\sigma_{120}^\theta)^2 \cdot \bar{u}_t^\theta(\frac{s}{2})] \tag{5}$$

From Eqs. (1), (4) and (5), we have,

$$W_{2N-N} = N \cdot \frac{1}{\sin \theta} (t_\theta)^2 \cdot \frac{1}{E_2} [(\sigma_{20}^\theta)^2 \{2\bar{u}_n^\theta(\frac{s}{2}) - \bar{u}_n^\theta(s)\} + (\sigma_{120}^\theta)^2 \{2\bar{u}_t^\theta(\frac{s}{2}) - \bar{u}_t^\theta(s)\}] \tag{6}$$

The formation of N new cracks in the presence of N existing cracks will be possible if the work required to form (or close) the cracks, supplied by the applied stress σ_{X0} , is sufficient to overcome the material resistance, i.e. if

$$W_{2N-N} \geq N \cdot W_c \cdot \frac{1}{\sin \theta} t_\theta \tag{7}$$

where W_c is the material resistance (energy) per unit crack plane area per unit laminate width. The quantity W_c is not necessarily the same as the familiar critical energy release rate G_c , which is associated with unstable growth of a crack tip. If the given crack advances by symmetric opening of the crack surfaces, then $G_c = G_{Ic}$, the mode I value, while $G_c = G_{IIc}$ or $G_c = G_{IIIc}$, if the crack surfaces slide past each other in mode II or mode III, respectively. In a mixed opening and sliding case, the instability of crack growth is determined by a combined resistance to crack growth.

In the damage scenario considered here, as described above and illustrated in Fig. 2, the newly formed cracks are identical in their size and shape to the pre-existing cracks. The crack tips (fronts) of the pre-existing as well as the new cracks are arrested at the ply interfaces between the off-axis plies and the adjacent plies. The process of crack multiplication (from N to $2N$ cracks) does not involve instability of crack tip advance. In fact, the exact process by which the new cracks form is not the object of interest here. Instead, we are interested in determining the value of the applied laminate stress at which the crack multiplication process is completed. Eq. (7) expresses the condition for completion of this process and the quantity W_c appearing there is to be interpreted as the total energy dissipated (per unit crack plane per unit laminate width) in completion of the said process.

Let us call the quantity W_c as the crack multiplication toughness and discuss it further. For an off-axis crack of the geometry considered here, let us denote the work terms in Eq. (6) as W_I and W_{II} associated with COD and CSD, respectively. Thus,

$$W_I = \frac{(\sigma_{20}^\theta)^2 t_\theta}{E_2} \left[2\tilde{u}_n^\theta \left(\frac{s}{2} \right) - \tilde{u}_n^\theta(s) \right],$$

$$W_{II} = \frac{(\sigma_{120}^\theta)^2 t_\theta}{E_2} \left[2\tilde{u}_t^\theta \left(\frac{s}{2} \right) - \tilde{u}_t^\theta(s) \right] \quad (8)$$

Analogous to the energy release rate for crack tip advance, let us write a criterion for crack multiplication as

$$\left(\frac{W_I}{W_{Ic}} \right)^a + \left(\frac{W_{II}}{W_{IIc}} \right)^b \geq 1 \quad (9)$$

where W_{Ic} and W_{IIc} are the crack multiplication toughness values in COD and CSD modes, respectively, and a and b are arbitrary constants.

Experimental data reported in Varna et al. (1999) on off-axis cracking in $[0/\pm\theta_4/0_{1/2}]_s$ laminates loaded in axial tension show that for angles $\theta = 40^\circ$ or less, no cracks initiated before laminate failure. Even for $\theta = 55^\circ$ the cracks did not form until the axial strain of 1.0%. These observations, coupled with the calculated ply stresses, suggest that unless the stress normal to fibers in the off-axis plies is tensile and sufficiently high, multiple cracks do not form. The shear stress in the plies by itself does not produce the off-axis cracks. For instance, ± 45 angle-ply laminate shows a nonlinear response but no ply cracking before failure although the in-plane shear stresses can be quite large. It therefore seems reasonable to infer that the crack multiplication toughness W_{IIc} is sufficiently high such that the second term in Eq. (9) can be neglected, leaving with the modified criterion as

$$\frac{W_I}{W_{Ic}} \geq 1 \quad (10)$$

In subsequent analysis of off-axis cracking we shall use this criterion, evaluating the W_{Ic} toughness from data on cross-ply laminates.

Using the first of Eq. (8) in Eq. (10) gives now the basis for relating the applied laminate stress σ_{x0} (or corresponding laminate strain ϵ_{x0}) to the crack spacing s (or crack density $1/s$) when the off-axis ply stress σ_{20}^θ is expressed in terms of σ_{x0} or ϵ_{x0} . This is done by employing the ply stress-strain relations

$$\begin{Bmatrix} \sigma_{10}^\theta \\ \sigma_{20}^\theta \\ \sigma_{120}^\theta \end{Bmatrix} = \begin{bmatrix} Q_{11} & Q_{12} & 0 \\ Q_{12} & Q_{22} & 0 \\ 0 & 0 & Q_{66} \end{bmatrix} \begin{Bmatrix} \epsilon_{10}^\theta \\ \epsilon_{20}^\theta \\ 2\epsilon_{120}^\theta \end{Bmatrix} \quad (11)$$

in conjunction with the strain transformation relations that relate the ply strains to the laminate strain, given by

$$\begin{Bmatrix} \epsilon_{10}^\theta \\ \epsilon_{20}^\theta \\ \epsilon_{120}^\theta \end{Bmatrix} = \begin{bmatrix} m^2 & n^2 & 2mn \\ n^2 & m^2 & -2mn \\ -mn & mn & m^2 - n^2 \end{bmatrix} \begin{Bmatrix} \epsilon_X \\ \epsilon_Y \\ \epsilon_{XY} \end{Bmatrix} \quad (12)$$

where $m = \cos \theta$; $n = \sin \theta$, and the stiffness coefficients in Eq. (11) are related to the ply elasticity constants by the following equations:

$$Q_{11} = \frac{E_1}{1 - \nu_{12}\nu_{21}}; \quad Q_{22} = \frac{E_2}{1 - \nu_{12}\nu_{21}};$$

$$Q_{11} = \frac{\nu_{12}E_2}{1 - \nu_{12}\nu_{21}}; \quad Q_{66} = G_{12} \quad (13)$$

Finally, we consider the *multiple cracking initiation strain* ϵ_{x0} defined as the applied laminate axial strain at which the cracking process begins. To estimate it, we assume that it is given by the limiting state of multiple cracking where the crack density approaches zero, or equivalently, the crack spacing approaches infinity. We derive it from the cracking criterion, Eq. (10), in which W_I is now the value given by Eq. (8) for $s \rightarrow \infty$, i.e.

$$W_I|_{s \rightarrow \infty} = \frac{(\sigma_{20}^\theta)^2 t_\theta}{E_2} \tilde{u}_n^\theta \Big|_{s \rightarrow \infty} \quad (14)$$

Thus we obtain, on using Eqs. (11)–(13),

$$\epsilon_{x0} = \frac{1}{\bar{Q}} \sqrt{\frac{E_2 W_{Ic}}{t_\theta \tilde{u}_n^\theta|_{s \rightarrow \infty}}};$$

$$\bar{Q} = Q_{12}(m^2 - \nu_{XY0}n^2) + Q_{22}(n^2 - \nu_{XY0}m^2) \quad (15)$$

where

$$\nu_{XY0} = -\frac{\epsilon_{Y0}}{\epsilon_{X0}} \quad (16)$$

which can be calculated using laminate theory for uncracked laminate.

2.1. Evaluation of crack multiplication toughness W_{Ic}

The crack multiplication toughness, as defined here, represents the energy dissipated per unit area in a series of failure processes as the laminate goes from State 1 (N cracks) to State 2 ($2N$ cracks). These failure processes consist of fiber/matrix debonding, matrix shear banding and failure, micro-crack formation and coalescence, ply crack growth through ply thickness and by tunneling in the width direction, etc. Above all, in the crack multiplication process, the stress transfer through the ply interfaces is involved. It is unrealistic to expect all energy dissipation in these events to be lumped together in a critical energy release rate parameter, which essentially represents the energy barrier that needs to be overcome in advancing a crack tip. We propose instead that W_{Ic} is viewed as a threshold of energy that needs to be crossed for completion of the crack multiplication process. Since the nature of events involved in the crack multiplication process depends on the presence of the constraining environment (plies adjacent to the cracking plies), e.g. in ply crack arrest at ply interfaces and in subsequent tunneling growth, W_{Ic} cannot truly be a material parameter but rather a laminate parameter, i.e. depending on the ply material as well as the stacking configuration of the laminate. Thus, we propose that W_{Ic} be evaluated in the context of a laminate. A procedure to evaluate this quantity will be described in Section 4.

3. FE modeling

As would be clear from the previous section, the prediction of ply cracking using Eq. (10) requires normalized average COD (\tilde{u}_n^θ) as a function of crack spacing s . To evaluate this quantity for various laminate configurations and crack densities, separate 3-D FE models were constructed for $[0/\pm\theta_4/0_{1/2}]_s$ and $[0_m/90_p/\mp\theta_n]_s$ laminates. Representative unit cells for the two laminate configurations along with symmetry boundary conditions are shown in Figs. 3 and 4. In FE analysis, the cell size is varied to determine CODs at varying crack density. The matrix cracks were assumed to have grown across the entire width of the specimen. ANSYS SOLID45 (eight-noded isoparametric) elements were used. A fine mesh was used in each FE model. Mapped meshing was utilized to flow the mesh smoothly through the thickness. Aspect ratio of elements near the crack surfaces was kept close to 1.0 for better accuracy. Linear Elastic FE analyses were carried out on unit cells using ANSYS (version 11.0) at 0.5% strain. Displacement boundary conditions were applied by constraining the left end of the unit cell and providing required displacement at the right end such that,

$$(u)_{X=0} = 0; \quad (u)_{X=2l} = u^0; \quad (w)_{Z=0} = 0 \quad (\text{symmetry}) \quad (17)$$

where $2l$ and u^0 represent the length of unit cell and the applied displacement, respectively, in the laminate longitudinal direction. It is

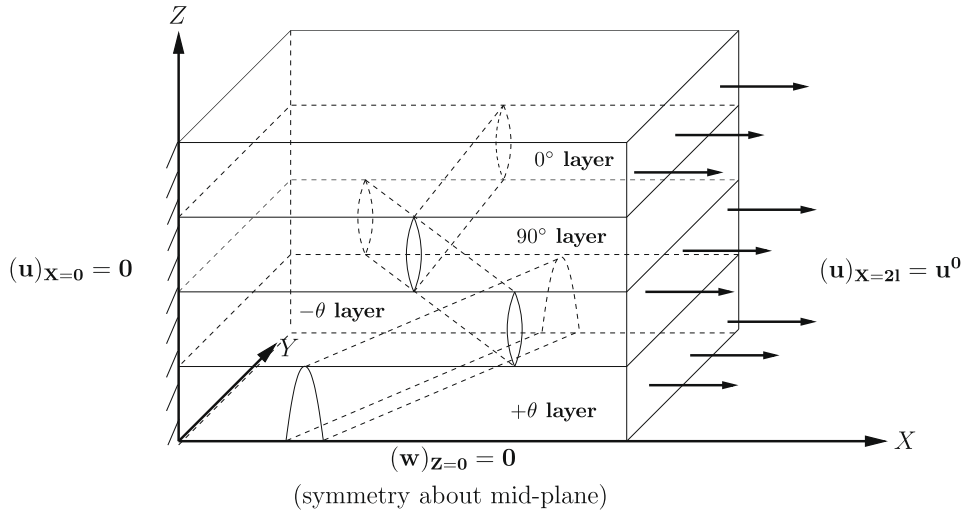


Fig. 3. A representative unit cell for FE analysis of $[0_m/90_p/\pm\theta_n]_s$ laminate.

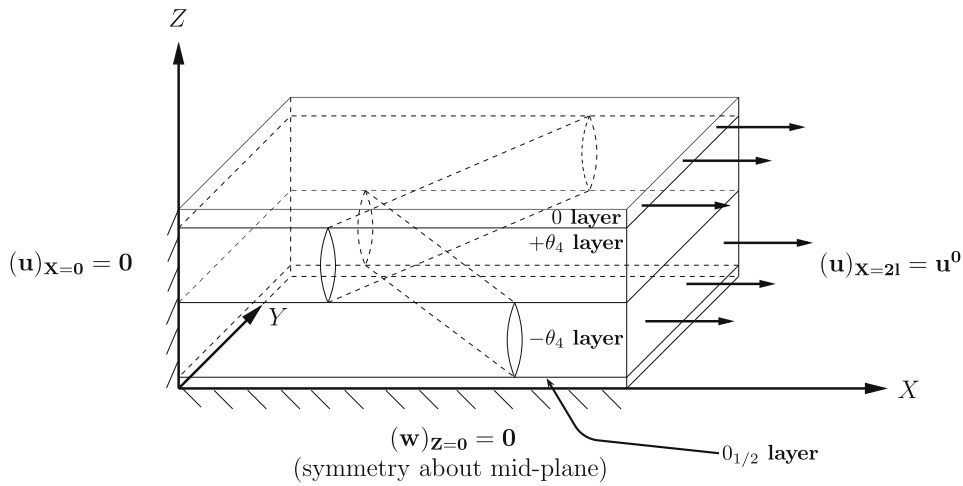


Fig. 4. A representative unit cell for FE analysis of $[0/\pm\theta_4/0_{1/2}]_s$ laminates.

noted that the above boundary conditions are specified in the laminate (global) coordinate system (X,Y,Z) . The local coordinate system on a crack plane is denoted by x_i , $i = 1, 2, 3$ as it is aligned with the lamina coordinate system (see Fig. 2).

Due to the presence of crack surfaces in three directions $(+\theta, -\theta$ and $90^\circ)$, it is not possible to construct a fully periodic unit cell for the cracked laminate. Since there is no periodicity in the width direction, the width of the unit cell is chosen large enough such that the errors due to effects from the free edges are negligible. Thus the cell used here is not a repeating unit cell, but a “representative” unit cell.

4. Analysis results

To illustrate the application of the energy model described in Section 2, we compare our predictions with the experimental data for two laminate configurations: $[0/\pm\theta_4/0_{1/2}]_s$ and quasi-isotropic $([0/90/\pm 45]_s)$, published by Varna et al. (1999) and Tong et al. (1997), respectively. We will then predict damage evolution for more general cases of $[0_m/90_p/\pm\theta_n]_s$ and $[0_m/\pm\theta_n/90_p]_s$ laminates, providing a limited parametric study of changes in layer thicknesses.

From FE simulations at a fixed crack spacing, the average COD is calculated as (Eq. (3))

$$\bar{u}_n^\theta = \frac{1}{t_0} \int_{-t_0/2}^{t_0/2} \Delta u_2(x_3) dx_3 \tag{18}$$

where $\Delta u_2 = u_2^+ - u_2^-$ represents the separation of crack planes in the direction normal to the crack face. As noted above, the coordinate x_2 is transverse to the fiber, in the local lamina coordinate system. Numerically, Δu_2 is determined from nodal x_2 -direction displacements averaged over the entire crack surface.

The complete procedure to implement the described energy model for the micro-crack initiation and evolution in an off-axis ply of a general symmetric laminate is outlined below. The procedure is in two parts:

Part I: estimate W_{lc}

1. From FE simulations, determine the variation of COD (Eq. (18)) with crack spacing.
2. Assume a value for W_{lc} . Plot damage evolution for the reference laminate by taking following steps:
 - (a) Divide specimen length in small intervals of length $\delta X = t_0/10$.
 - (b) Find the multiple crack initiation strain using Eq. (15).
 - (c) Assume a small initial crack density, e.g. $\rho_{initial} = \frac{1}{50t_0}$ chosen here.

- (d) Choose a random length interval and check for cracking. A new crack forms when criterion set in Eq. (10) is satisfied. Increase crack density and eliminate the cracked length interval from further consideration for ply cracking.
 - (e) Choose another length interval and repeat previous step till fracture criterion is satisfied.
 - (f) Increase applied strain. Repeat steps (d) and (e) at this strain value.
3. Iterate Step 2 by varying W_{Ic} so that the resulting evolution curve fits the experimental data for the reference laminate. For example, for predicting damage evolution in $[0/\pm\theta_4/0_{1/2}]_s$ laminates, we chose $[0/90_8/0_{1/2}]_s$ as the reference laminate.

Part II: predict damage evolution for other off-axis plies

1. From FE simulations, determine the variation of COD (Eq. (18)) with crack spacing for a given off-axis laminate.
2. Using the value for W_{Ic} obtained above, predict damage evolution by following steps 2(a)–(f) described in Part I.

4.1. Quasi-isotropic ($[0/90/\mp 45]_s$) laminates

The ply properties for this case are: ply thickness = 0.5 mm, $E_1 = 46$ GPa, $E_2 = 13$ GPa, $G_{12} = 5$ GPa and $\nu_{12} = 0.3$. To obtain the remaining properties for use in the 3-D model, the unidirectional ply is assumed transversely isotropic in the cross-sectional plane. Thus, the properties related to thickness direction are taken as: $E_3 = E_2 = 12$ GPa; $G_{13} = G_{12} = 5$ GPa; $\nu_{13} = \nu_{12} = 0.3$; $\nu_{23} = 0.4$ (assumed), and $G_{23} = \frac{E_3}{2(1+\nu_{23})} = 4.3$ GPa.

Normalized average COD values obtained from FE simulations for this case are shown in Fig. 5 for reference cross-ply ($[0/90]_s$) and quasi-isotropic ($[0/90/\mp 45]_s$) laminates. As the crack density increases, COD decreases due to interaction between nearby cracks in a given layer. To enable representation of COD as a continuous function of crack density, polynomial fits to the calculated data were used in numerical simulations predicting damage evolution.

The choice of a reference laminate for this class of laminate configuration is less obvious. Ideally, a reference laminate should allow calibration of the crack multiplication toughness W_{Ic} for that laminate configuration, i.e. reflect dependence on ply material as well as the stacking configuration of the laminate, as stated in Section 2.1. For example, a reference laminate could be $[0/90/-30/+30]_s$, i.e. $m = 1$, $n = 1$, $p = 1$, $\theta = 30^\circ$. The model would then predict

damage evolution for other values of m , n , p and θ . If this reference laminate were chosen, experimental data would be required for it. However, the source in the literature that had data for $[0/90/\mp 45]_s$ also had data for $[0/90]_s$ laminate. We chose therefore to calibrate W_{Ic} for the latter laminate and make prediction of damage evolution in the former.

In the first step, the damage evolution model is calibrated with the experimental data for the reference $[0/90]_s$ glass-epoxy laminate to yield the value of W_{Ic} . This value is found to be 232 J/m² and it is utilized to predict the damage progression in $[0/90/\mp 45]_s$ laminates, as shown in Fig. 6. For determination of strain to initiate ply cracking, COD value extrapolated for zero crack density is utilized in Eq. (15). In general, the model predictions are in good agreement with the experimental data. The important point to consider is the ply cracking process in quasi-isotropic laminates in comparison to cross-ply laminates. The cracks initiate always first in the 90° layer at about 0.5% applied strain for both cross-ply and quasi-isotropic layups. However, the crack density at saturation is higher in the quasi-isotropic laminate than in the cross-ply laminate. The broken line in the figure shows the evolution of ply cracks in the 90° layer when there are no ply cracks in -45° and $+45^\circ$ layers. This is true initially during the loading process. However, at high levels of loading, cracks appear also in -45° and $+45^\circ$ layers, causing a slight increase in the rate of damage evolution in the 90° ply. During experiments, Tong et al. (1997) observed that the ply cracks initiate in -45° layer at the interface where 90° cracks meet the -45° layer. Later, cracks develop in $+45^\circ$ layer at the intersection of developed -45° -cracks and $-45^\circ/+45^\circ$ interface. These cracks, however, do not progress fully in the laminate width before other damage modes (delaminations, etc.) appear. As reported in our previous paper (Singh and Talreja, 2009), cracks in -45° and $+45^\circ$ layers cause only a small degradation in the stiffness of the whole laminate.

4.2. $[0/\pm\theta_4/0_{1/2}]_s$ laminates

Each ply in the present laminate configuration is 0.125 mm thick. The ply material is glass-epoxy (HyE 9082Af, Fiberite) with in-plane properties $E_1 = 44.7$ GPa, $E_2 = 12.7$ GPa, $G_{12} = 5.8$ GPa and $\nu_{12} = 0.297$. Similar to Section 4.1, transverse isotropy in third direction is assumed to obtain 3D properties. The calculated COD values for this case are plotted in Fig. 7.

For these laminates it was observed that the direct use of fracture criterion in Eq. (10) does not predict the rate of damage evolution consistent with the experiments. This aspect of damage

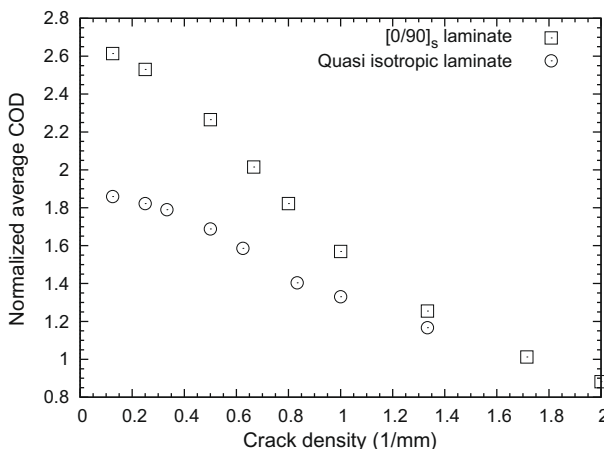


Fig. 5. Variation of normalized average COD for 90° -cracks with crack density for $[0/90]_s$ and $[0/90/\mp 45]_s$ laminates.

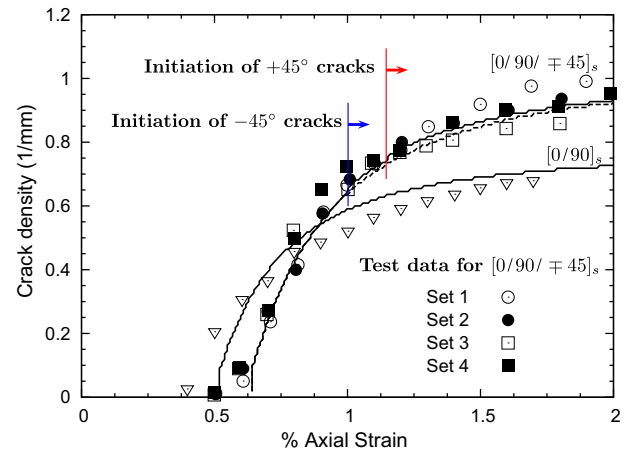


Fig. 6. Evolution of 90° -crack density in $[0/90]_s$ and $[0/90/\mp 45]_s$ laminates. The experimental data are from Tong et al. (1997).

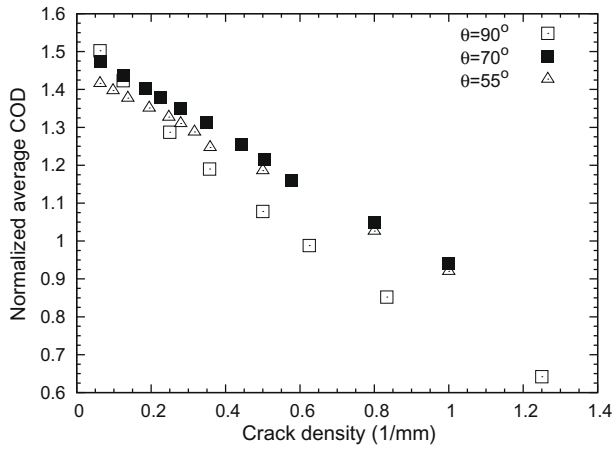


Fig. 7. Variation of normalized average COD with crack density for $[0/\pm\theta_4/0_{1/2}]_s$ laminates ($\theta = 90^\circ, 70^\circ,$ and 55°).

evolution modeling has earlier been observed in the literature (e.g. Liu and Nairn, 1992; Vinogradov and Hashin, 2005). The basic argument is that at low crack densities, the work W_I is almost constant. However, on development of sufficient cracks with a distribution in inter-crack spacing, it will be a function of this spacing. To account for this behavior, Liu and Nairn (1992) suggested that introducing the concept of an effective crack spacing, which results in the modified W_I as follows:

$$W_I = \frac{(\sigma_{20}^0)^2 t_\theta}{E_2} \left[2\tilde{u}_n^0\left(\frac{fs}{2}\right) - \tilde{u}_n^0(fs) \right] \quad (19)$$

where f is the average ratio of the crack interval in which a micro-crack forms to the average crack spacing. For cross-ply laminates, they found that $1.2 < f < 1.5$ fits well with their experimental data. However, for $[0/\pm\theta_4/0_{1/2}]_s$ laminate we find that $f = 0.8$ predicts damage evolution plot closest to the experimental data. Fig. 8 shows comparisons between predictions and experimental data for the $[0/90_8/0_{1/2}]_s$ laminate and forms the basis for calibration of W_{Ic} and f .

In the present case, W_{Ic} is determined to be 212 J/m^2 . It is slightly less than the value obtained above for $[0/90]_s$ laminate probably due to difference in lamina thickness and the processing methods for the two laminates. Once we have determined W_{Ic} , we can now predict damage progression in the other off-axis laminates following the damage procedure described in Section 2.

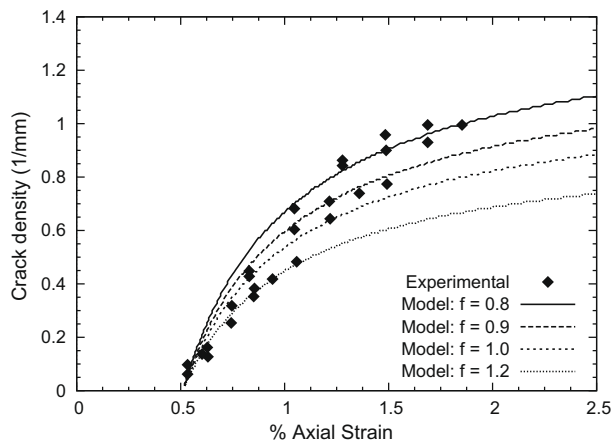


Fig. 8. Determination of fitting parameter f and crack multiplication toughness W_{Ic} using experimental data for $[0/90_8/0_{1/2}]_s$ laminate. The experimental data are from Varna et al. (1999).

Fig. 9 compares the model predictions for crack initiation strains and the experimental data (Varna et al., 1999). For ply orientations close to 90° , the strain to initiate crack increases gradually as θ decreases. However, for $\theta < 60^\circ$, this strain increases more rapidly and below 40° , we observe that the model predicts extremely high strains to cause ply cracking. For all practical purposes, this implies that the cracks cannot form for low ply orientations. These predictions are consistent with the experimental results on other off-axis laminates (Crocker et al., 1997; Tong et al., 1997; Varna et al., 1999).

Using $f = 0.8$, the plots of crack density evolution for $[0/\pm 70_4/0_{1/2}]_s$ and $[0/\pm 55_4/0_{1/2}]_s$ laminates, are shown in Figs. 10 and 11, respectively. The predictions show reasonable correspondence with the experimental data. In case of $\theta = 70^\circ$, the damage model does not match with experimental measurements at high crack densities likely because of initiation of delamination in the laminate specimen. For $\theta = 55^\circ$, the experimental data showed significant coupon-to-coupon variation (Varna et al., 1999), as seen in the two sets of the reported experimental data.

4.3. $[0_m/90_n/\mp\theta_p]_s$ laminates

As discussed in Section 4.1, damage in the case of quasi-isotropic laminates is primarily due to the 90° -cracking. However, for

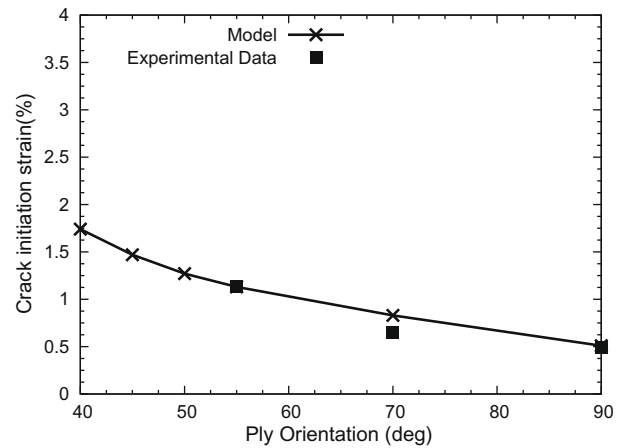


Fig. 9. Comparison of crack initiation strains with experimental data (Varna et al., 1999) for $[0/\pm\theta_4/0_{1/2}]_s$ laminates.

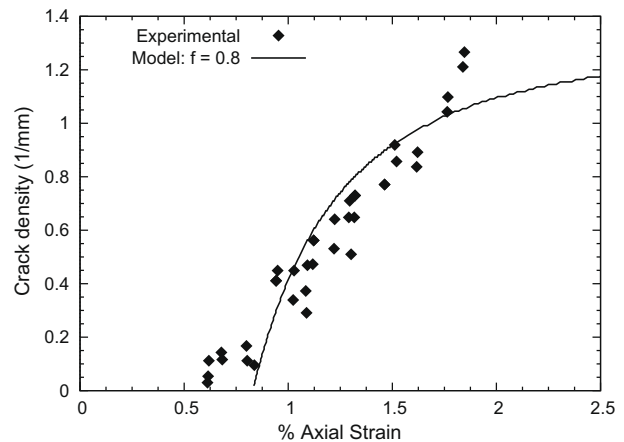


Fig. 10. Damage evolution in $[0/\pm 70_4/0_{1/2}]_s$ laminates. The experimental data are from Varna et al. (1999). The crack density is average of crack densities in $+70^\circ$ and -70° plies.

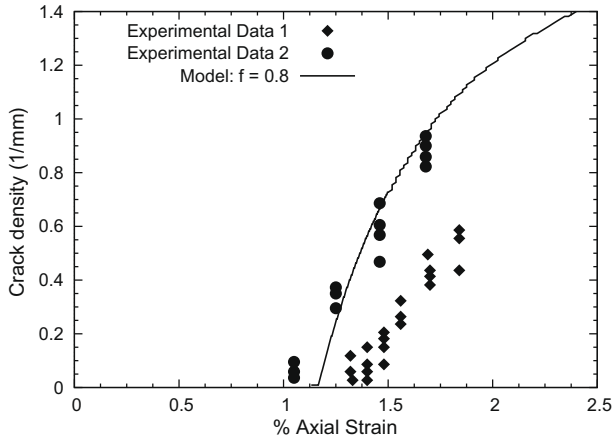


Fig. 11. Damage evolution in $[0/\pm 55_4/0_{1/2}]_s$ laminates. The experimental data are from Varna et al. (1999). The crack density is average of crack densities in $+55^\circ$ and -55° plies.

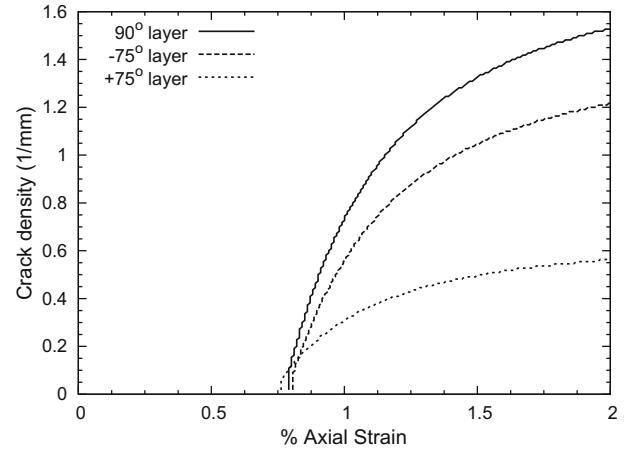


Fig. 13. Damage evolution in $[0/90/\mp 75]_s$ laminates.

$[0_m/90_n/\mp \theta_p]_s$ laminates with θ close to 90° , $\mp\theta$ -modes could also be significant and consequently there could be important interactions between the two damage modes. The crack density of these damage modes can be predicted by computing CODs when both crack systems are incorporated in the laminate FE analysis. Note that this interaction between damage modes is appreciable only when θ is close to 90° .

The ply properties and W_{ic} for these laminates are assumed to be same as those for the quasi-isotropic laminate discussed in Section 4.1. The damage progression predictions with applied axial strain for $[0/90/\mp 60]_s$ and $[0/90/\mp 75]_s$ laminates are shown in Figs. 12 and 13. For $\theta = 60^\circ$, 90° -cracks were predicted to form first. 90° -cracks then help in initiation and progression of $\mp 60^\circ$ -cracks from the interface between $\mp 60^\circ$ and 90° -layers. Hence, initially in the simulation only 90° -mode is active till $\mp 60^\circ$ -cracks form. However, for $\theta = 75^\circ$, both damage modes are found to initiate at almost the same applied strain; hence all modes are active initially in the FE simulation.

4.4. $[0_m/90_n/\mp \theta_p]_s$ vs. $[0_m/\pm \theta_p/90_n]_s$ laminates

It is known that in a laminate with a mix of on-axis and off-axis plies, such as $[0_m/\pm \theta_p/90_n]_s$ laminate, the in-plane elastic properties are not affected by a change in the ply stacking sequence if the relative proportion of the plies of any orientation is kept the same.

Thus this particular laminate will keep its in-plane elastic properties in a configuration given by $[0_m/90_n/\mp \theta_p]_s$. However, such change of the ply stacking sequence can significantly affect the initiation and progression of multiple ply cracking. We shall demonstrate this by taking one example where $\theta = 60^\circ$. The damage evolution curves for the $[0/90/\mp 60]_s$ and $[0/\pm 60/90]_s$ laminates are depicted in Figs. 12 and 14, respectively, where the crack densities of each of the three ply orientations are shown against the applied laminate strain. Significant differences in both the initiation strain and the saturation crack density values are seen.

4.5. Parametric study of layer thickness

The procedure for predicting damage progression described here can also be used for other laminates of the type $[0_m/90_n/\mp \theta_p]_s$. With change in cracked/uncracked ply thicknesses, CODs computed from FE simulation also change and they affect the damage initiation and progression accordingly. As the thickness of a cracked layer is increased, the applied strain to initiate cracking in that layer, as well as in other cracking layers, decreases. On the other hand, increase in thickness of uncracked supporting plies increases the crack initiation strain.

The first case considered here is $[0_m/90_n/\mp 45_p]_s$ laminate. For this laminate configuration, fully grown cracks are assumed only in 90° layer. Predicted damage evolution curves for 90° -cracking for different values of m , n and p are shown in Fig. 15. It is clearly

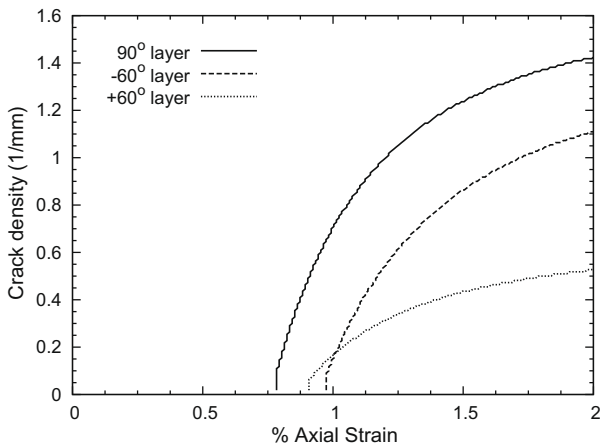


Fig. 12. Damage evolution in $[0/90/\mp 60]_s$ laminates.

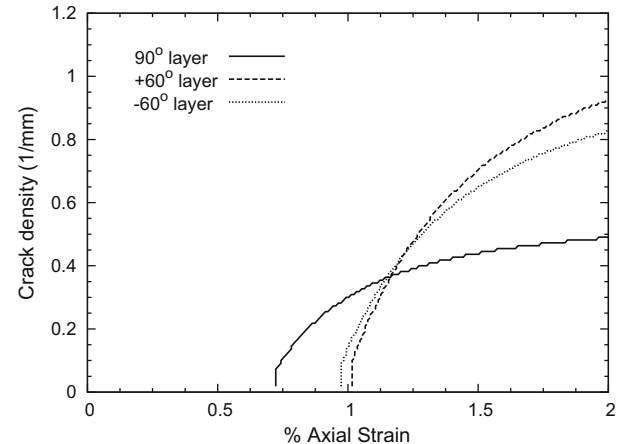


Fig. 14. Damage evolution in $[0/\pm 60/90]_s$ laminates.

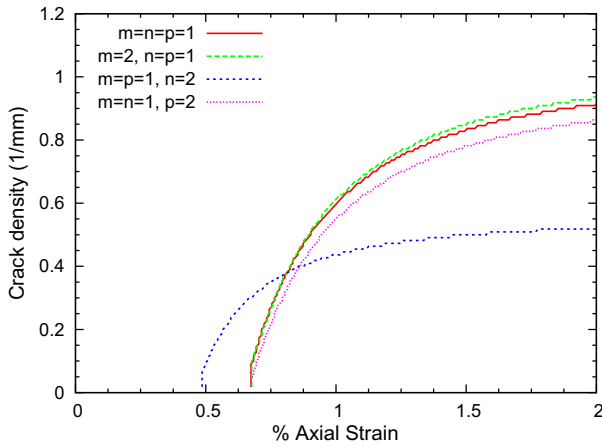


Fig. 15. Damage evolution for 90°-cracking in $[0_m/90_n/\pm 45_p]_s$ laminates.

seen that the crack initiation strains are almost the same for $m = n = p = 1$, $m = 2$, and $p = 2$, whereas for $n = 2$, crack initiation strain decreases to below 0.5% as compared to 0.66% for $m = n = p = 1$. Also, the shape of evolution curve is influenced by the relative number of plies in a specific orientation. As the thickness of 90°-layer is doubled, the saturation crack density is nearly halved. However, change in thickness of other layers does not affect the saturation crack density significantly.

The second case refers to $[0_m/90_n/\mp 60_p]_s$ laminates. In this case, cracks usually initiate in 90° first and then in $\mp 60^\circ$ layers. Thus, initial simulation assumes only 90° cracks; whereas after the initiation of $\mp 60^\circ$ cracks, a multi-mode scenario is used in FE modeling. As described earlier, $\mp 60^\circ$ cracks influence the damage progression in 90° layer. The predictions for different m, n, p values are shown in Fig. 16(a)–(c) for 90°, -60° and $+60^\circ$ layers, respectively. For $p = 2$, the model predicts that cracks in the -60° and $+60^\circ$ layers will initiate earlier than in the 90° layer.

The final case is for damage progression in $[0_m/90_n/\mp 75_p]_s$ laminates. In this scenario, cracks can initiate in all cracking layers almost at the same applied strain. Hence, all modes of damage could be present simultaneously. The predictions for this laminate are shown in Fig. 17(a)–(c) for 90°, -75° and $+75^\circ$ layers, respectively. Observations similar to the above can be made with regards to crack initiation strain, shape of evolution curve and the saturation cracks density.

5. Discussion

5.1. Choice of representative cell

For laminates with cracking in multiple layers with different orientations, the relative density of cracks and their relative positions in respective layers dictate the choice of representative unit cell for COD computation, as discussed below.

1. *Relative position of cracks:* Experimental observations suggest that cracks in differentially oriented plies begin at their common interface, e.g. in quasi-isotropic $[0/90/-45/45]_s$ laminates (Tong et al., 1997) cracks in $\pm 45^\circ$ plies grew from the interface between these plies and the 90°-plies at the points where the 90°-cracks met the interface. Similarly, the $+45^\circ$ -cracks initiated at the locations where -45° -cracks met the $-45^\circ/+45^\circ$ interface. When the cracks in different orientations are sufficiently closely spaced to cause additional perturbation in the ply stress fields on top of that due to cracking in those plies, the FE model for the representative unit cell must con-

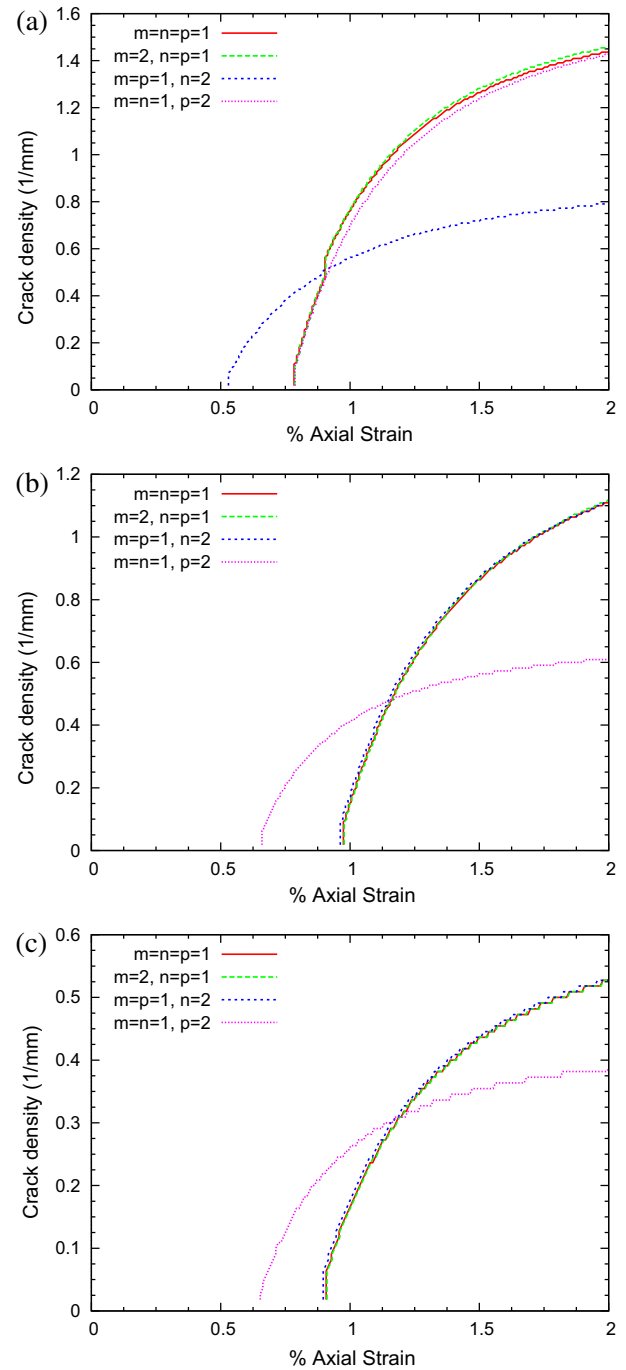


Fig. 16. Damage evolution in $[0_m/90_n/\mp 60_p]_s$ laminates: (a) 90° layer, (b) -60° layer, and (c) $+60^\circ$ layer.

sider all plies cracked at the same time (see for example Fig. 3). Otherwise, the interactions between differently oriented cracks can be neglected, as illustrated in Fig. 18.

2. *Relative density:* The length of the representative unit cell is dictated by the cracking mode with minimum crack density (i.e. the maximum crack spacing). For example, the representative unit cell for $[0/90/\pm \theta]_s$ laminate with relative crack densities equal to $\rho_{+\theta}/\rho_{90} = \rho_{-\theta}/\rho_{90} = 1/3$ must consider three cracks in 90° ply and one crack each in $+\theta$ and $-\theta$ plies, as shown in Fig. 19 for the maximum interaction case. In case the relative densities are not in integral multiples, the unit cell construction is not straightforward. Li et al. (2009) have treated this case. We

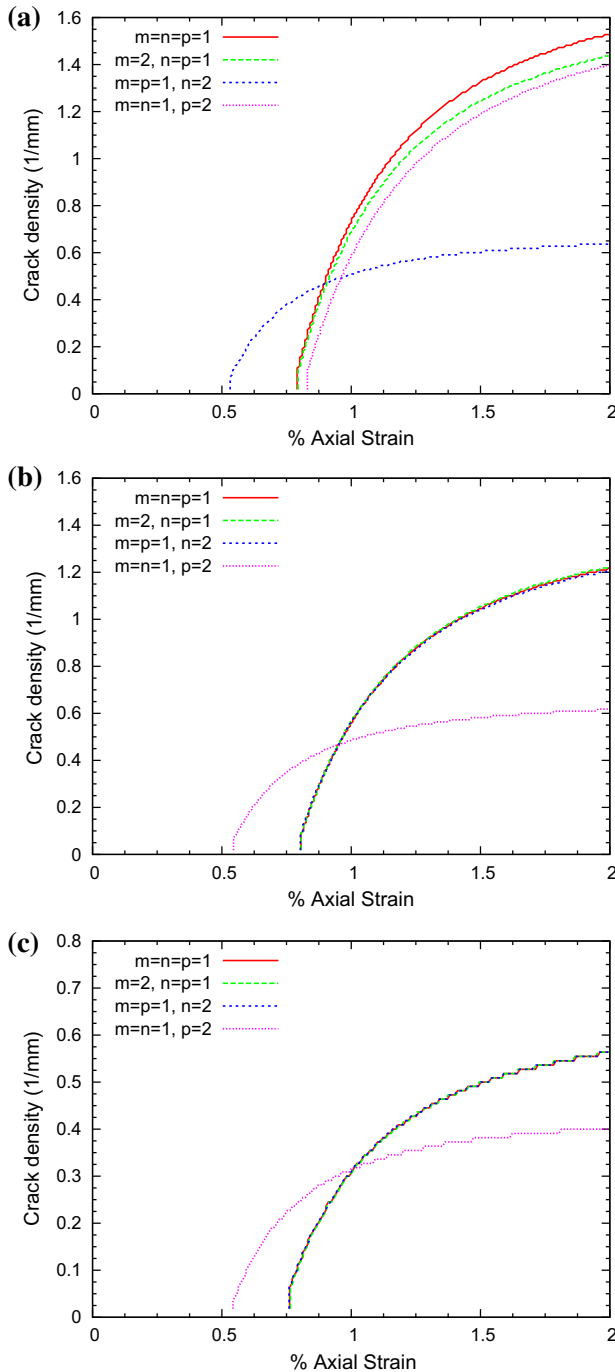


Fig. 17. Damage evolution in $[0_m/90_n/\mp 75_p]_s$ laminates: (a) 90° layer, (b) -75° layer, and (c) $+75^\circ$ layer.

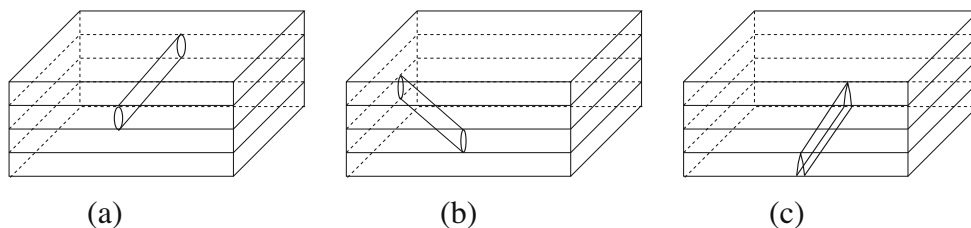


Fig. 18. FE models for COD computation in $[0/90/+ \theta/- \theta]_s$ laminate for non-interactive case with: (a) 90° cracks only, (b) $+ \theta$ cracks only, and (c) $- \theta$ cracks only.

considered here the $[0/-60/45/-60/45/0]_s$ laminate with crack spacing in the outer -60° at three times that of in the inner -60° ply, and crack spacing in the outer 45° ply at half the crack spacing in the inner 45° ply. The locations of cracks in different plies are thus staggered with an offset, as shown in Fig. 20.

5.2. Shape of damage evolution curve

Fig. 21 depicts the actual and predicted shape of the damage evolution curve. The ply cracking phenomenon usually comprises three stages. Stage I corresponds to the formation of initial matrix cracks and their propagation through the specimen thickness and width. In most cases, transverse matrix cracks initiate at the edge of the specimen and quickly traverse the thickness direction. However, depending upon the ply orientations, these cracks may or may not propagate instantaneously through the whole laminate width. For cross-ply laminates, this through-width propagation is facilitated by the fact that propagation direction is normal to the loading direction and as a result, the cracks propagate almost instantaneously (at the experimental time scale), and are sometimes called *tunneling cracks*. This instant propagation of cracks in the laminate width direction may not occur for other ply configurations. It also depends upon the quality of the coupons. If specimens are well prepared, they will have few flaws and will show a rapid rise in crack density just after first micro-crack formation (Nairn, 2000). Stages II and III in the plot correspond to the increase in density of ply cracks. In the beginning of Stage II, these cracks are not equally spaced due to randomness of the material resistance to fracture. However, in the later part of this stage, these cracks form roughly periodic arrays. Stage III represents slowing down of crack multiplication rate due to mutual crack interaction, leading to a saturation state. Since the damage model discussed here does not account for crack propagation through laminate thickness and width, it cannot accurately predict Stage I of the curve. Also, the damage model will predict axial strain at first crack formation as the extrapolated lower limit of Stage II.

5.3. Limitations of the model

The predictive methodology presented here for ply cracking evolution in multiple orientations has been simplified by neglecting the contribution of crack surface sliding to the work of crack multiplication. This allows calibrating the crack multiplication toughness for a given laminate configuration from experimental data obtained on a reference laminate with transverse cracks only. The predictions by this procedure have given reasonable correspondence with experimental data for other laminates. More experimental data would allow further assessment of the accuracy of the prediction procedure. It is noted, however, that the observed crack density values near saturation can be affected by delaminations that are not accounted for in the model.

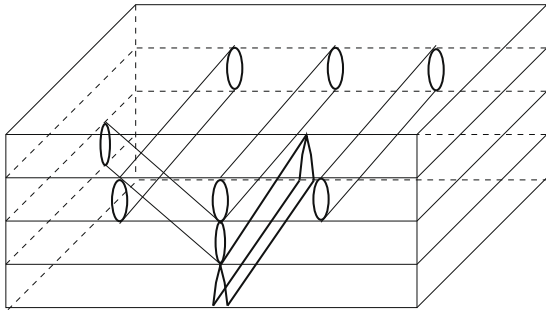


Fig. 19. FE model for COD computation in $[0/90/+ \theta/ - \theta]_s$ laminate for maximum intra-mode interaction with relative crack density of 3:1:1 in 90° , $+ \theta$, and $- \theta$ layers, respectively.

Since the variation in the crack spacing is significant mostly in the early stage of cracking, the assessment of the correction parameter is approximate. The accuracy of this assessment depends also on the scatter in the data. Further work is needed to develop a more accurate procedure for evaluating the crack multiplication toughness.

6. Conclusions

We have considered the problem of matrix crack multiplication in off-axis plies of laminates subjected to axial tensile load. Based on physical observations, parallel array of intralaminar cracks with their planes aligned with the ply thickness direction have been assumed. The crack multiplication process has been further assumed to be “self-similar” in the sense that pre-existing equally spaced N cracks are assumed to multiply to $2N$ cracks without changing their geometry.

An energy-based approach has been taken where it is postulated that a critical value of the work to open the cracks is needed to form additional cracks in the presence of pre-existing cracks. Thus, when cracks are in other than the 90° plies, the work to conduct crack sliding displacement is assumed not to be critical for crack formation. This simplifying assumption has been found to predict the damage evolution reasonably well. Any loss in accuracy by this simplification can be justified by not having to determine the critical value of work needed to form cracks in shear.

The critical work to form new ply cracks in the presence of pre-existing cracks, called crack multiplication toughness here, has been viewed as a laminate property, and for a given class of laminate configuration, such as $[0/\pm \theta_4/0_{1/2}]_s$, it is evaluated from the evolution data for the 90° -ply cracking case. The prediction of damage evolution in other cases for the same laminate configuration, based on this value, has been found to be in reasonable correspondence with the test data.

The parametric study of evolution of three sets of cracks, in $+ \theta$ plies, $- \theta$ plies and 90° -plies, in the $[0_m/90_n/\mp \theta_p]_s$ laminate configuration has revealed that the crack density saturation occurs at the highest level for 90° -plies followed by the $- \theta$ plies and the $+ \theta$ plies. The damage evolution picture is altered significantly if the 90° -plies are moved to the middle. In general, the damage initiation and progression in an off-axis orientation depend on the local constraint on the crack opening displacement imposed by the plies immediately surrounding the cracking plies. The total thickness

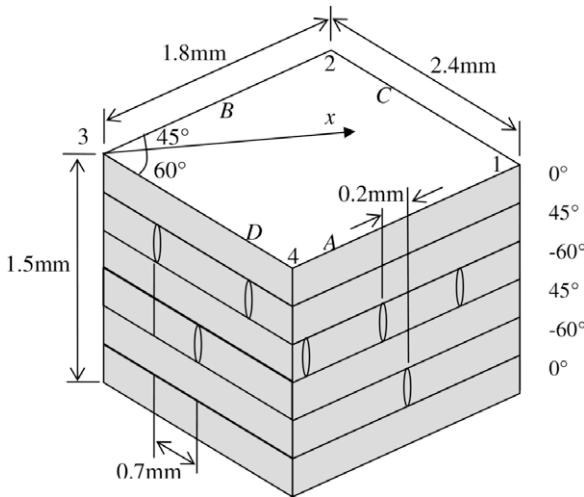


Fig. 20. An example of representative unit cell for cracking in $[0/-60/45/-60/45/0]_s$ laminate with unequal crack densities in different layers, reprinted from Li et al. (2009).

In evaluating the crack multiplication toughness a correction parameter has been used along the lines of Liu and Nairn (1992) to account for the varying crack spacing in the experimental data versus uniform crack spacing assumed in the model.

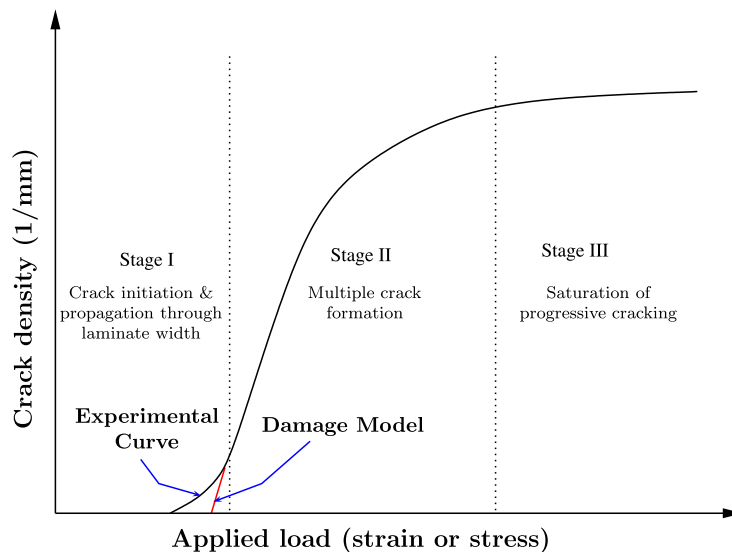


Fig. 21. A typical damage evolution curve for transverse matrix cracking in composite laminates.

of the unseparated plies in an off-axis orientation is also found to be important in the damage evolution process.

References

- Berthelot, J.M., 2003. Transverse cracking and delamination in cross-ply glass-fiber and carbon-fiber reinforced plastic laminates: static and fatigue loading. *Appl. Mech. Rev.* 56 (1), 111–147.
- Crocker, L.E., Ogin, S.L., Smith, P.A., Hill, P.S., 1997. Intra-laminar fracture in angle-ply laminates. *Composites A* 28 (9–10), 839–846.
- Irwin, G., 1958. *Handbuch der Physik VI*. Springer, Berlin, pp. 551–590 (Chapter: Fracture I).
- Joffe, R., Krasnikovs, A., Varna, J., 2001. Cod-based simulation of transverse cracking and stiffness reduction in $[s/90_n]_s$ laminates. *Compos. Sci. Technol.* 61 (5), 637–656.
- Kashtalyan, M., Soutis, C., 2006. Modelling off-axis ply matrix cracking in continuous fibre-reinforced polymer matrix composite laminates. *J. Mater. Sci.* 41 (20), 6789–6799.
- Li, S., Singh, C.V., Talreja, R., 2009. A representative volume element based on translational symmetries for fe analysis of cracked laminates with two arrays of cracks. *Int. J. Solids Struct.* 46, 1793–1804.
- Liu, S.L., Nairn, J.A., 1992. The formation and propagation of matrix microcracks in cross-ply laminates during static loading. *J. Reinforced Plast. Compos.* 11 (2), 158–178.
- Nairn, J.A., 2000. Matrix microcracking in composites. In: Talreja, R., Manson, J.A.E. (Eds.), *Polymer Matrix Composites*, vol. 2. Elsevier, Amsterdam, pp. 403–432.
- Nairn, J.A., Hu, S.F., Bark, J.S., 1993. A critical-evaluation of theories for predicting microcracking in composite laminates. *J. Mater. Sci.* 28 (18), 5099–5111.
- Singh, C.V., Talreja, R., 2008. Analysis of multiple off-axis ply cracks in composite laminates. *Int. J. Solids Struct.* 45 (16), 4574–4589.
- Singh, C.V., Talreja, R., 2009. A synergistic damage mechanics approach for composite laminates with matrix cracks in multiple orientations. *Mech. Mater.* 41, 954–968.
- Tong, J., Guild, F.J., Ogin, S.L., Smith, P.A., 1997. On matrix crack growth in quasi-isotropic laminates – I. Experimental investigation. *Compos. Sci. Technol.* 57 (11), 1527–1535.
- Varna, J., Joffe, R., Akshantala, N.V., Talreja, R., 1999. Damage in composite laminates with off-axis plies. *Compos. Sci. Technol.* 59 (14), 2139–2147.
- Vinogradov, V., Hashin, Z., 2005. Probabilistic energy based model for prediction of transverse cracking in cross-ply laminates. *Int. J. Solids Struct.* 42 (2), 365–392.
- Yang, T.L., Liu, Y.B., Wang, J., 2003. A study of the propagation of an embedded crack in a composite laminate of finite thickness. *Compos. Struct.* 59 (4), 473–479.
- Yokozeki, T., Aoki, T., Ogasawara, T., Ishikawa, T., 2005. Effects of layup angle and ply thickness on matrix crack interaction in contiguous plies of composite laminates. *Composites A* 36 (9), 1229–1235.